REPORT DOCUMENTATION PAGE

Form Approved OMB NO. 0704-0188

1. REPORT DATE (DD-MM-YYYY)	2. REPORT TYPE	3. DATES COVERED (From - To)
14-02-2022	Final Report	25-Jan-2019 - 30-Jun-2021

4. TITLE AND SUBTITLE
Final Report: On-Chip Frequency Comb Generation at Visible Wavelengths Using III-Nitride Photonic Integrated Circuits

5a. CONTRACT NUMBER
W911NF-19-1-0089

5b. GRANT NUMBER

5c. PROGRAM ELEMENT NUMBER
611103

6. AUTHORS

5d. PROJECT NUMBER

5e. TASK NUMBER

5f. WORK UNIT NUMBER

7. PERFORMING ORGANIZATION NAMES AND ADDRESSES

Arizona State University
ORSPA
P.O. Box 876011
Tempe, AZ 85287 -6011

8. PERFORMING ORGANIZATION REPORT NUMBER

9. SPONSORING/MONITORING AGENCY NAME(S) AND ADDRESS (ES)

U.S. Army Research Office
P.O. Box 12211
Research Triangle Park, NC 27709-2211

10. SPONSOR/MONITOR'S ACRONYM(S)
ARO

11. SPONSOR/MONITOR'S REPORT NUMBER(S)
69667-EL-PCS.5

12. DISTRIBUTION AVAILIBILITY STATEMENT

Approved for public release; distribution is unlimited.

13. SUPPLEMENTARY NOTES

The views, opinions and/or findings contained in this report are those of the author(s) and should not contrued as an official Department of the Army position, policy or decision, unless so designated by other documentation.

14. ABSTRACT

15. SUBJECT TERMS

16. SECURITY CLASSIFICATION OF:			17. LIMITATION OF ABSTRACT	15. NUMBER OF PAGES	19a. NAME OF RESPONSIBLE PERSON
a. REPORT	b. ABSTRACT	c. THIS PAGE			Yuji Zhao
UU	UU	UU	UU		19b. TELEPHONE NUMBER 713-348-4392

RPPR Final Report
as of 22-Feb-2022

Agency Code: 21XD

Proposal Number: 69667ELPCS **Agreement Number: W911NF-19-1-0089**
INVESTIGATOR(S):

Name: Yuji Zhao
Email: yuji.zhao@rice.edu
Phone Number: 7133484392
Principal: Y

Organization: **Arizona State University**
Address: ORSPA, Tempe, AZ 852876011
Country: USA
DUNS Number: 943360412 EIN: 860196696

Report Date: 30-Sep-2021 Date Received: 14-Feb-2022
Final Report for Period Beginning 25-Jan-2019 and Ending 30-Jun-2021

Title: On-Chip Frequency Comb Generation at Visible Wavelengths Using III-Nitride Photonic Integrated Circuits
Begin Performance Period: 25-Jan-2019 **End Performance Period:** 30-Jun-2021
Report Term: 0-Other

Submitted By: Yuji Zhao Email: yuji.zhao@rice.edu
Phone: (713) 348-4392

Distribution Statement: 1-Approved for public release; distribution is unlimited.

STEM Degrees: 1 **STEM Participants:**

Major Goals: The overarching goal of this research plan is to elucidate fundamental physical mechanisms that hinder development of optical micro-combs, and demonstrate that novel materials and optical engineering can be successfully applied to fabrication of on-chip optical frequency combs at visible wavelengths using III-nitride photonics integrated circuit (PIC). Three specific objectives are planned to explore the theoretical and experimental aspects of this innovative photonics platform:

1. Investigate hitherto unexplored fundamental optical processes in III-nitride photonics including photonic crystals (PhCs) structures, four-wave mixing (FWM) processes, and group velocity dispersion (GVD) properties.

2. Tackle engineering obstacles presented by MOCVD growth and nanofabrication to achieve a III-nitride PIC, consisting of (i) an InGaN-based continuous wave (CW) green LD; (ii) a AlN-based PhC resonator operating at visible wavelengths, which is the first of its kind; and (iii) AlN waveguides.

3. Demonstrate the world's first on-chip visible micro-comb using III-nitride PIC, thus marking an important advancement towards realizing on-chip visible and UV optical combs, which can significantly enhance the state of the art in optical computing and bio-chemical sensing applications.

Proposed here is a pathway towards on-chip optical frequency comb generation that uses an innovative photonic platform (III-nitride PIC), with the potential to transform the foundations of existing frequency comb technology. For example, the proposed III-nitride PIC will enable the development of hitherto unachievable visible and UV micro-combs for on-chip optical computing and for bio-chemical sensing applications, which are critical to the DoD mission. Long-term, the study is expected to advance basic knowledge in III-nitride photonics including PhC, laser physics, and nonlinear optics, all of which are essential to the design and fabrication of other III-nitride PIC components, such as photodetectors, optical modulators, and optical logic gates, all of which again are attractive for a range of mission-critical DoD defense applications.

Accomplishments: 1. Visible spectrum frequency comb via supercontinuum generation.
To achieve frequency comb generation that covers visible spectrum, one promising approach is to exploit near-visible (800 nm) pumping and perturb the soliton by third order dispersion. The near-visible spectrum pumping allows nonlinear optical energy transfer from infrared (IR) to visible spectrum at high energy efficiency. Solitons perturbed by third order dispersion provides directional energy transfer through non-solitonic radiation. As a result, the broadband frequency comb can be obtained. To achieve this target, we fabricated high performance AlN waveguides, and successfully excited a high order mode (TE10) within a micro photonic waveguide, which provides

anomalous dispersion in the pumping wavelength region. The narrow spectra frequency comb pumping source was obtained from a mode locked Ti:Sapphire laser (Spectra-physics, Tsunami), and the output spectrum was collected by an optical spectrum analyzer (Yokogawa, AQ6373B). Additionally, numerical solvers were also built for the modeling of frequency combs. The spectral evolution of short pulse was modeled by the in-house made nonlinear Schrodinger's equation (NSE) solvers, and the waveguide propagation loss was estimated by in-house made dyadic Green's functions (DGF).

By carefully adjusting the dispersion parameters, anomalous dispersion was obtained with a zero-dispersion wavelength near 750 nm. By pumping the device at the wavelength at 810 nm, a broadband frequency comb was obtained with a main spectrum covering from 490 nm to 1100 nm. Since the AlN possesses non-zero second order susceptibility, a secondary spectrum from 405 nm to 425 nm was also observed from the second harmonic generation. Due to the near-zero-dispersion wavelength pumping, only ~0.36 nJ pulse energy within TE10 mode was required. To the best of our knowledge, this is the first on-chip demonstration that covers the most portion of visible spectrum wavelengths. Numerical simulation was also performed to investigate the broadening mechanism, and the outcome of pulse spectral evolution agrees well with our hypothesis that the spectrum was broadened by soliton fission through third order dispersion within TE10 mode. Additionally, to confirm the coherence the broadband outcome spectrum, shot noise was added onto the numerical simulation, good coherence was maintained, indicating that the broadening process preserves the phase coherence. The recorded spectrum and numerical simulation are provided the Figs. 1 to 3. These results were published in two journal papers in ACS Photonics and Nanophotonics, and were presented in international conferences such as CLEO and ICNS.

2. UV spectrum using QPM method
To further expand the spectrum obtained from previous results into ultraviolet (UV) region, we explore the quasi-phase matching (QPM) method, which is achieved by periodically modifying the waveguide width. When QPM is used in the second harmonic generation (SHG). The second order susceptibility will periodically change its sign, which allows for continuous growth of harmonically generated optical power. When QPM is used in the soliton fission, it will periodically modify the group velocity dispersion (GVD) and the high orders of dispersion terms. Our results show that the phase matched points will extend further into the UV region of the spectrum, which is beneficial for supercontinuum generation to cover the full UV-visible spectrum.

To investigate the QPM techniques, we simulated various periodically modified waveguide structures and the results are shown in Figs. 4 and 5. When waveguide geometry was modulated, the dispersion of the soliton split into different orders, which led to the phase matching at different orders. When no loss was applied, a 30 nm of broadening can be observed from 480 nm to 450 nm. When loss was applied, QPM generated frequency component was still observable. These results were published in two journal papers in ACS Photonics and Nanophotonics, and were presented in international conferences such as CLEO and ICNS.

3. Coherence estimation of supercontinuum spectrum
We used a first-order coherent function to numerically estimate the coherence of supercontinuum spectrum on our AlN devices. The simulation takes 100 supercontinuum pulses with a standard shot noise at the input spectra, and the noise spectrum is constituted by one photon per spectral bin. Using our home-built first-order coherent function simulation tool, we also calculated the coherence of supercontinuum spectrum under different relative intensity noise (RIN), and the results are shown in Fig. 6. When no RIN was applied, the coherence function was close to unity. When RIN was within MHz frequency range or THz frequency range, the RIN originated from fluctuations between or within the pulses, both of which affected the coherence function of the devices. The simulation suggests that the internal power fluctuation of every single pulse is of crucial importance in achieving coherent supercontinuum generations. These results were published in two journal papers in ACS Photonics and Nanophotonics, and were presented in international conferences such as CLEO and ICNS.

4. Fabrication of AlN low loss waveguide
To analysis the loss mechanisms, we developed a numerical model to evaluate the defect scattering from III-nitride waveguides. Since III-nitride thin films grown on sapphire substrates are accompanied with high density of threading dislocations, the outcome of this research highlights the importance of MOCVD growth and suggests that threading dislocation (TD) density over 1010 (cm−2) would induce significant scattering loss. Fig. 7 shows the simulation results. During the study, we also found out that because our current AlN devices are fabricated on sapphire substrates, the SiO_2 coating layers that we used will result in asymmetric refractive index profiles in the devices, which is detrimental for photonic crystal structures. To solve this issue, we optimized the fabrication processes by introducing a new coating layers of ALD deposited Al_2O_3 thin films, and replacing the original SiO_2 coating with the SiO_xN_y coating. After the ICP etching of AlN, an Al_2O_3 thin layer was deposited using ALD.

Thanks to the excellent uniformity of ALD, this thin layer provided full coverage on the etched sidewall, which passivated the dangling bonds and reduced the trap states at the surface. Then, the cladding layer of SiOxNy was deposited. We properly modified the PECVD recipe so that the index of SiOxNy matched with the index of sapphire substrate. These results were published in one journal paper in Optics Express, and were presented in international conferences such as CLEO and ICNS.

5. Low Loss Ga2O3 waveguide
Recently a new class of wide band gap semiconductor beta-phase gallium oxide (β-Ga2O3) has emerged with many promising properties. β-Ga2O3 possesses a bandgap energy of 4.8 eV and exhibits large laser induced damage threshold, which is promising for high power integrated photonic devices from UV to infrared (IR). The low refractive index contrast between the core and the cladding layers will also minimize the scattering loss in the devices. β-Ga2O3 also has a small lattice mismatch with the InAlGaN material system, which leads to the possible active integration of Ga2O3 photonic devices with InAlGaN lasers and detectors. Despite these attractive properties, there is no research efforts on β-Ga2O3 photonic devices, and their optical performance is largely unknown. In this period, we fabricated β-Ga2O3 waveguide devices and characterized their optical loss performance. We developed a chlorine based inductively coupled plasma etching method, which led to the smooth waveguide sidewall and reduced the loss in β-Ga2O3 devices. Four different laser wavelengths were used to measure the propagation loss from 810 nm to 400 nm. When the guide mode was propagat

Training Opportunities: One student Hong Chen finished his Ph.D. Thesis under the grant. The details are as follows.

Hong Chen, “Nonlinear integrated photonics in the visible spectrum based on III-N material platform”, Arizona State University, Ph.D. Thesis, May 2020.
*This thesis received Palais Outstanding Doctoral Student Award, which is the highest honor for ASU ECEE Ph.D. thesis with 1 awardee annually.

RPPR Final Report
as of 22-Feb-2022

Results Dissemination: 1. Journal Publications.
1). H. Chen, J. Zhou, D. Li, D. Chen, A. K. Vinod, H. Fu, X. Huang, T. H. Yang, J. Montes, K. Fu, C. Yang, C. Z. Ning, C. W. Wong, A. M. Armani, and Y. Zhao, “Supercontinuum generation in high order waveguide mode with near visible pumping using AlN waveguides”, ACS Photonics 8, 1344 (2021).

2). J. He, H. Chen, J. Hu, J. Zhou, Y. Zhang, A. Kovach, C. Sideris, M. C. Harrison, Y. Zhao, and A. M. Armani, “Nonlinear Nanophotonics devices in the ultraviolet to visible wavelength range”, Nanophotonics 8, 1344 (2020).

3). J. Zhou, H. Chen, H. Fu, K. Fu, X. Deng, X. Huang, T. H. Yang, J. A. Montes, C. Yang, X. Qi, B. Zhang, X. Zhang, and Y. Zhao, “Demonstration of low loss ?-Ga2O3 optical waveguides in the UV–NIR spectra”, Applied Physics Letters 115, 251108 (2019).

4). H. Chen, H. Fu, J. Zhou, X. Huang, T. H. Yang, K. Fu, C. Yang, J. A. Montes, and Y. Zhao, “Study of crystalline defect induced optical scattering loss inside photonic waveguides in UV–visible spectral wavelengths using volume current method”, Optics Express 27, 17262 (2019).

2. Conference Presentations.

1). J. Zhou, H. Chen, H. Fu, K. Fu, X. Deng, X. Huang, T. H. Yang, J. A. Montes, C. Yang, X. Qi, B. Zhang, X. Zhang, and Y. Zhao, “Demonstration of low loss ?-Ga2O3 optical waveguides in the UV–NIR spectra”, 2020 CLEO, May 2020, San Jose, CA, Poster Presentation.

2). J. Zhou, H. Chen, H. Fu, K. Fu, X. Deng, X. Huang, T. H. Yang, J. A. Montes, C. Yang, X. Qi, B. Zhang, X. Zhang, and Y. Zhao, “Demonstration of low loss ?-Ga2O3 optical waveguides in the UV–visible spectra”, 2020 MRS Spring Meeting, Apr 2020, Phoenix, AZ, Oral Presentation.

3). H. Chen, H. Fu, X. Huang, J. Zhou, T. H. Yang, K. Fu, J. Montes, C. Yang, and Y. Zhao, “Supercontinuum generation from dispersion engineered AlN waveguide arrays”, The 13th International Conference on Nitride Semiconductors 2019 (ICNS-13), Jul 2019, Bellevue, WA, Oral Presentation.

4). H. Chen, J. Zhou, T. H. Yang, H. Fu, J. Montes, X. Huang, K. Fu, J. Montes, C. Yang, and Y. Zhao, “Study of optical scattering loss induced by crystalline defects inside AlN waveguides using volume current method”, The 13th International Conference on Nitride Semiconductors 2019 (ICNS-13), Jul 2019, Bellevue, WA, Oral Presentation.

5). H. Chen, J. Zhou, H. Fu, X. Huang, T. H. Yang, K. Fu, J. Montes, C. Yang, and Y. Zhao, “Supercontinuum generation from dispersion engineered AlN nanophotonic waveguide arrays,” CLEO 2019, May 2020, San Jose, CA, Oral Presentation.

6). H. Chen, J. Zhou, H. Fu, X. Huang, and Y. Zhao, “Study of crystalline defect induced optical scattering loss inside AlN waveguides in UV-visible spectral wavelengths”, CLEO 2019, May 2020, San Jose, CA, Oral Presentation.

Honors and Awards: Nothing to Report

Protocol Activity Status:

Technology Transfer: Nothing to Report

PARTICIPANTS:

Participant Type: PD/PI
Participant: Yuji Zhao
Person Months Worked: 2.00 **Funding Support:**
Project Contribution:
National Academy Member: N

RPPR Final Report
as of 22-Feb-2022

Participant Type: Graduate Student (research assistant)
Participant: Jingan Zhou
Person Months Worked: 12.00 **Funding Support:**
Project Contribution:
National Academy Member: N

Participant Type: Graduate Student (research assistant)
Participant: Hong Chen
Person Months Worked: 12.00 **Funding Support:**
Project Contribution:
National Academy Member: N

ARTICLES:

Publication Type: Journal Article Peer Reviewed: Y **Publication Status:** 1-Published
Journal: Optics Express
Publication Identifier Type: DOI Publication Identifier: 10.1364/OE.27.017262
Volume: 27 Issue: 12 First Page #: 17262
Date Submitted: 8/30/19 12:00AM Date Published: 6/1/19 12:00AM
Publication Location:
Article Title: Study of crystalline defect induced optical scattering loss inside photonic waveguides in UV–visible spectral wavelengths using volume current method
Authors: Hong Chen, Houqiang Fu, Jingan Zhou, Xuanqi Huang, Tsung-Han Yang, Kai Fu, Chen Yang, Jossue A
Keywords: Finite element method, Quantum optics, Ring resonators, Spatial frequency, Wave propagation, X ray diffraction
Abstract: In this work, we study the crystalline defect induced optical scattering loss inside photonic waveguide. Volume current method is implemented with a close form of dyadic Green's function derived. More specifically, threading dislocation induced scattering loss inside AlN waveguides in UV–visible spectrum wavelengths are studied since this material is intrinsically accompanied with high densities of dislocations. The results from this study reveal that threading dislocations contribute significant amount of scattering loss when material is not MOCVD grown. Additionally, the scattering loss is strongly dependent on polarization and waveguide geometries: TM modes exhibit higher scattering loss compared with TE modes, and the multimode large core waveguides are more susceptible to threading dislocations compared with single mode waveguides and high- aspect-ratio waveguides. Conclusions from this work can be supported by several recently published inves
Distribution Statement: 3-Distribution authorized to U.S. Government Agencies and their contractors
Acknowledged Federal Support: **Y**

RPPR Final Report
as of 22-Feb-2022

Publication Type: Journal Article Peer Reviewed: Y **Publication Status:** 1-Published
Journal: Applied Physics Letters
Publication Identifier Type: DOI Publication Identifier: 10.1063/1.5133845
Volume: 115 Issue: 25 First Page #: 251108
Date Submitted: 8/7/20 12:00AM Date Published: 12/1/19 7:00AM
Publication Location:
Article Title: Demonstration of low loss b-Ga2O3 optical waveguides in the UV–NIR spectra
Authors: Jingan Zhou, Hong Chen, Houqiang Fu, Kai Fu, Xuguang Deng, Xuanqi Huang, Tsung-Han Yang, Jossı
Keywords: thin films, oxide, surface scattering, photon absorption, visible spectra, optical properties
Abstract: In this paper, we report the fabrication of low loss beta-phase gallium oxide (?-Ga2O3) optical waveguides and the propagation loss analysis of the waveguides in the ultraviolet (UV) to near infrared (NIR) spectral region. The ?-Ga2O3 thin films were grown on sapphire substrates using metal organic chemical vapor deposition and were fabricated into various waveguide structures using nanofabrication processes. A low propagation loss of 3.7?dB/cm was obtained on the ?-Ga2O3 waveguide at the wavelength of 810?nm, which is comparable to the state of the art. Combined with theoretical simulations, various loss mechanisms from two-photon absorption, sidewall scattering, top surface scattering, and bulk scattering were discussed for ?-Ga2O3 waveguides, and their contributions to the total optical loss were estimated. These results show that ?-Ga2O3 is a promising optical material for the fabrication of various integrated photonic devices in the UV–NIR spectra region.
Distribution Statement: 2-Distribution Limited to U.S. Government agencies only; report contains proprietary info
Acknowledged Federal Support: **Y**

CONFERENCE PAPERS:

Publication Type: Conference Paper or Presentation **Publication Status:** 1-Published
Conference Name: CLEO: Science and Innovations
Date Received: 30-Aug-2019 Conference Date: 05-May-2019 Date Published: 10-May-2019
Conference Location: San Jose, California
Paper Title: Supercontinuum Generation from Dispersion Engineered AlN Nanophotonic Waveguide Arrays
Authors: Hong Chen, Jingan Zhou, Houqiang Fu, Xuanqi Huang, Tsung-Han Yang, Kai Fu, Jossue A. Montes, Cł
Acknowledged Federal Support: **Y**

Publication Type: Conference Paper or Presentation **Publication Status:** 1-Published
Conference Name: CLEO: Applications and Technology
Date Received: 30-Aug-2019 Conference Date: 05-May-2019 Date Published: 10-May-2019
Conference Location: San Jose, California
Paper Title: Study of Crystalline Defect Induced Optical Scattering Loss inside AlN Waveguides in UV-Visible Spectral Wavelengths
Authors: Hong Chen, Jingan Zhou, Houqiang Fu, Xuanqi Huang, and Yuji Zhao
Acknowledged Federal Support: **Y**

RPPR Final Report
as of 22-Feb-2022

Partners

,

I certify that the information in the report is complete and accurate:
Signature: Yuji Zhao
Signature Date: 2/14/22 2:35PM

Final Technical Report

On-Chip Frequency Comb Generation at Visible Wavelengths Using III-Nitride Photonic Integrated Circuits

Army Research Office (ARO) PECASE Grant No. W911NF-19-1-0089
ARO Program Manager: michael.d.gerhold.civ@army.mil
PI: Yuji Zhao, Arizona State University (Tempe, AZ), yuji.zhao@asu.edu

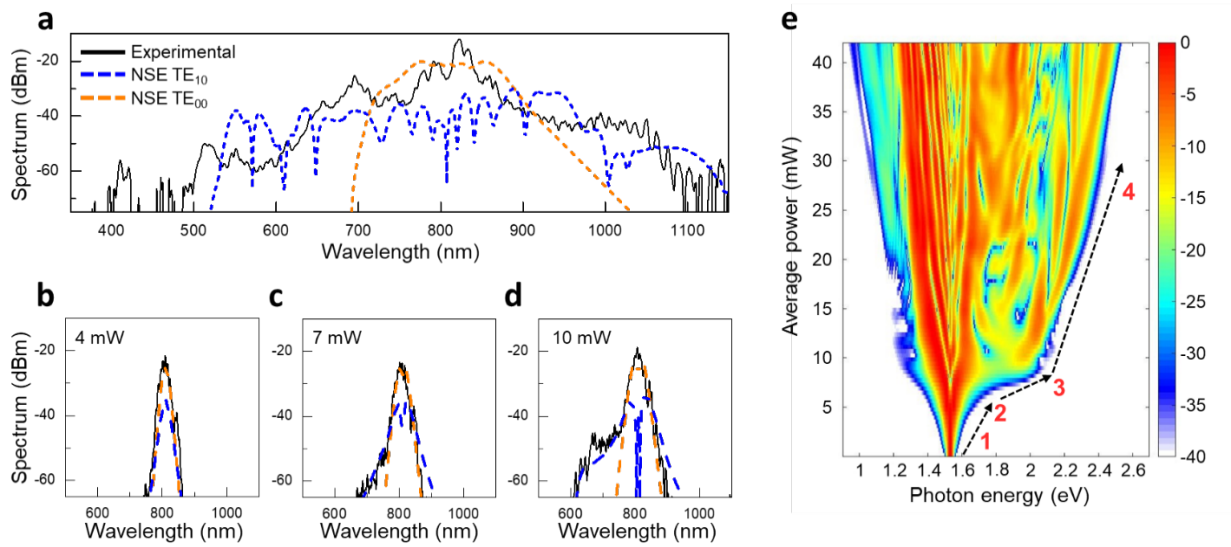

Fig. 1. (a) Experimental results of the obtained spectrum (black curve) at average pumping power of 30 mW (0.36 nJ pulse energy). Orange dash curve indicates the NSE solution of supercontinuum generation from TE00 mode. Blue dash curve indicates the NSE solution for TE10 mode. The experimentally recorded spectrum is composed by TE00 and TE10 spectrum. (b-d) Spectral evolution at different pumping power. (b) Under the average power of 4 mW, the broadening is mainly caused by self-phase modulation. (c) Above the average power of 7 mW, asymmetric broadening start to initiate due to the soliton fission through 3rd order dispersion. (d) Strong asymmetric broadening at average power of 10 mW. (e) Simulated spectrum evolution of TE10 mode. From point 1 to point 4, the recorded spectrum is corresponding to (b), (c), (d), and (a), respectively.

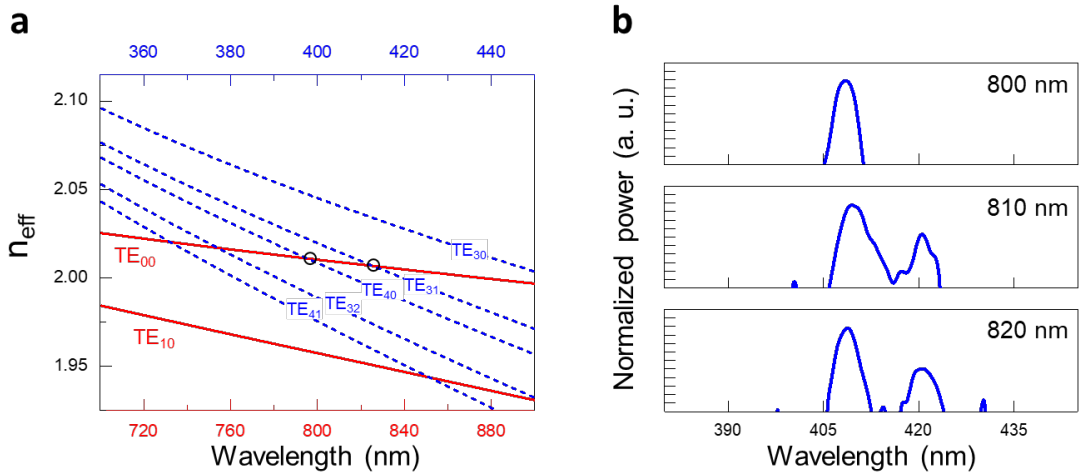

Fig. 2. (a) Calculated modal dispersion curves for TE00 and TE10 mode near fundamental wavelengths (800 nm), and the dispersion curves for high order modes near second harmonic generated wavelengths (400 nm). The two phase-matched points can be identified to be near 398 nm and 411 nm, marked out by black solid circles. (b) Experimentally recorded second harmonic spectrum at different pumping wavelengths. Two peaks can be identified at 408 nm and 421 nm, which agrees well with simulations. The small discrepancy can be attributed to varied waveguide geometry during fabrication processes. The locations of two peaks are independent of pumping wavelengths, which also suggests that the secondary spectrum is obtained by phase-matched process.

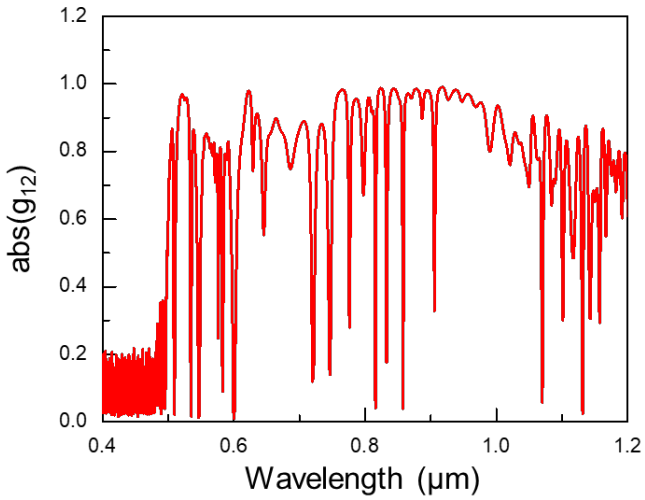

Fig. 3. The simulated coherence function (g12). 100 pulses are recorded independently with standard short noise involved. The coherence function can be obtained by calculating the ensemble average of electric filed. The coherence function is above 0.8 across a broadband spectrum, which suggests that the phase coherence can be well preserved during the broadening process.

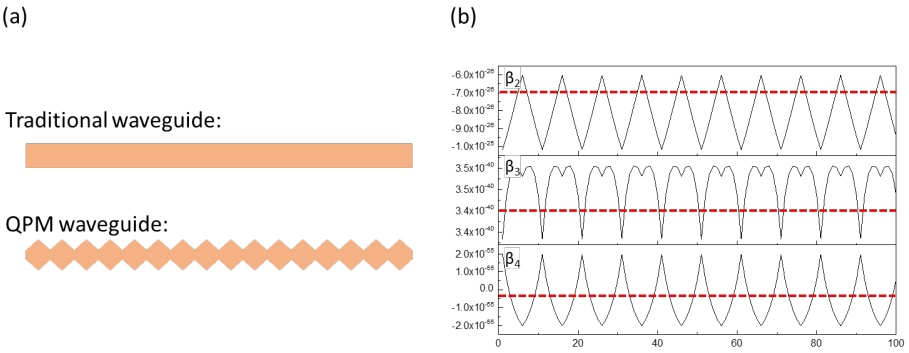

Fig. 4. The concept of QPM techniques. (a) Waveguide geometries for traditional waveguide and QPM waveguide. (b) The modulated second order, third order, and fourth order dispersions versus propagation distance.

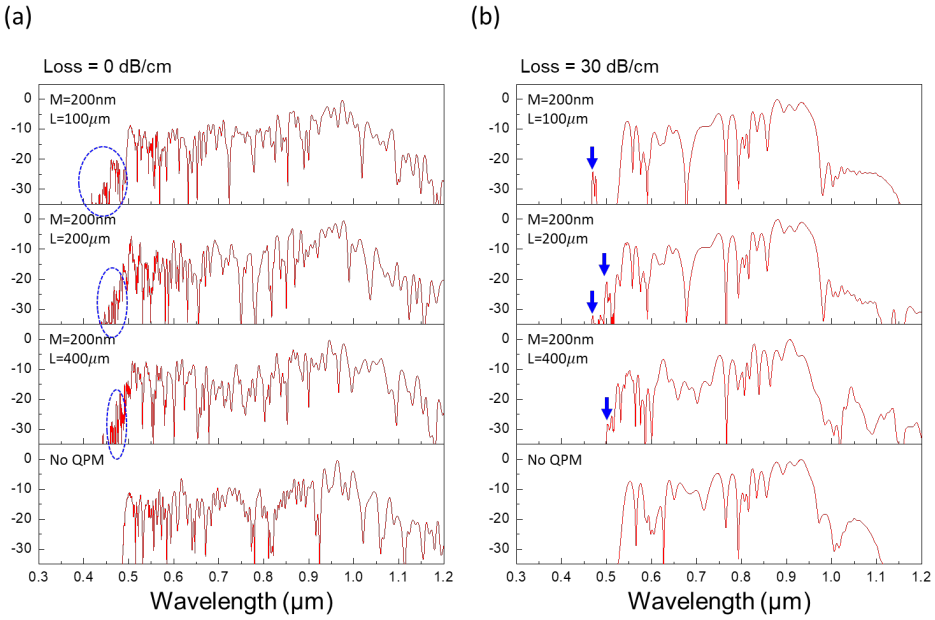

Fig. 5. The NSE simulated spectrum at different period and modulation depth. (a) The obtained spectrum when loss is not applied. The QPM generated wavelengths are marked by blue dash circles. (b) 30 dB/cm of loss was applied, the QPM signal can still be identified as marked by blue arrows.

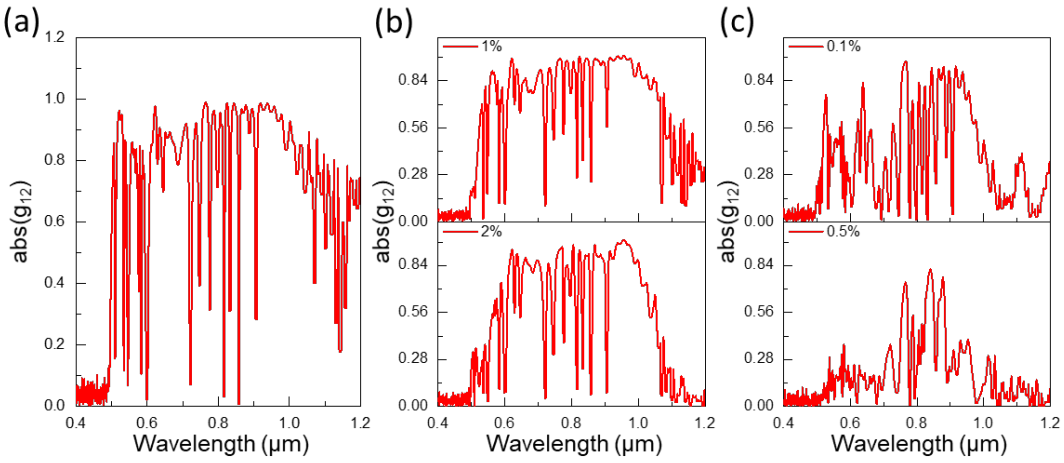

Fig. 6. The simulated first-order coherence function vs. wavelengths for AlN waveguide with a width of 1.2 μm at different noise conditions. (a) quantum limited shot noise involved. (b) shot noise plus 1% (top) and 2% (bottom) intra-pulse RIN (MHz level). (c) shot noise plus 0.1% (top) and 0.5% (bottom) inter-pulse power fluctuation.

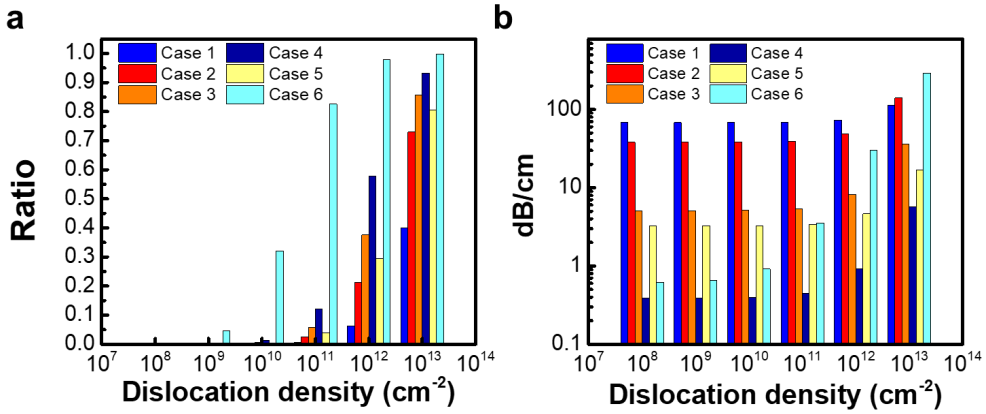

Fig. 7. (a) Calculated ratio between defect scattering loss and total loss versus dislocation density. (b) Total loss in dB/cm at different dislocation densities. For MOCVD grown thin films, the dislocation density is below 10^{10}, which indicates that the defect scattering does not contribute significant loss in MOCVD grown samples. The sputtered AlN thin films typically exhibit dislocation density above 10^10, where defect scattering becomes influential to the waveguide performance.

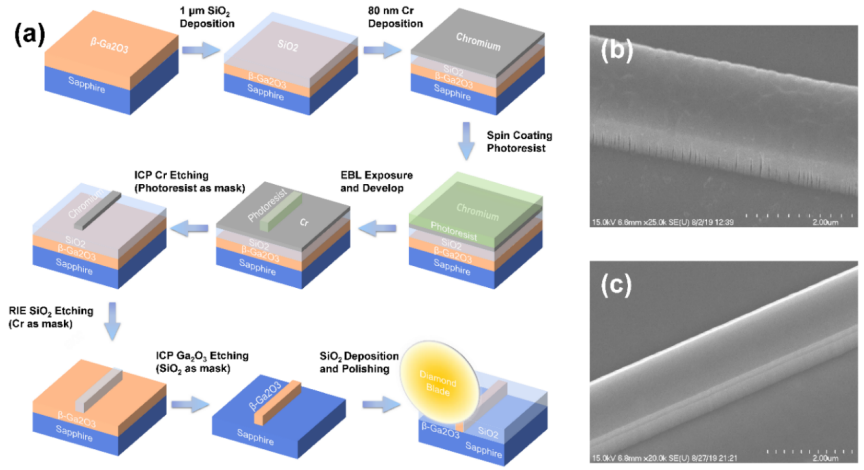

Fig. 8. (a) Schematics of the fabrication process for β-Ga_2O_3 waveguides. (b) SEM images of waveguide sidewall with unoptimized ICP recipe. (c) SEM images of waveguide sidewall with optimized ICP recipe.

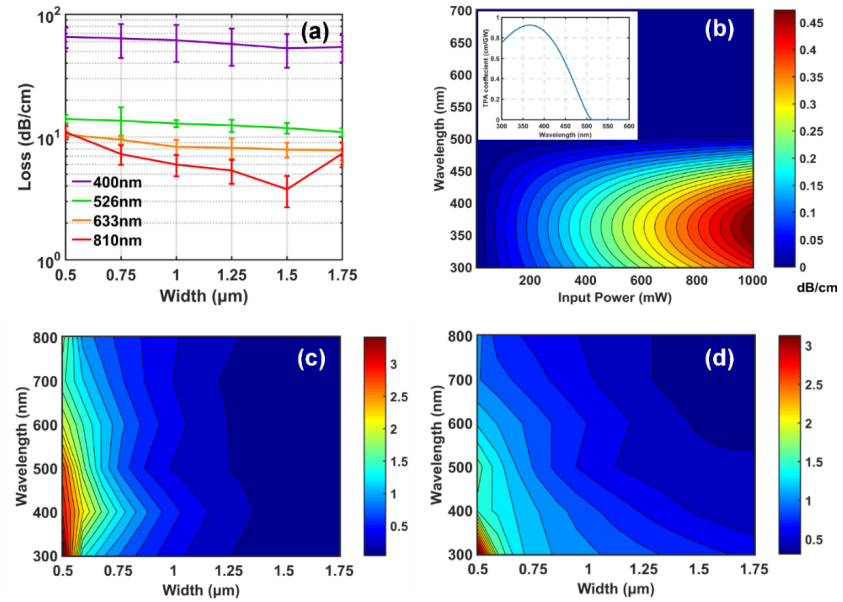

Fig. 9. (a) Measured propagation loss of β-Ga_2O_3 waveguides with different widths at different wavelengths. (b) Calculated TPA loss for β-Ga_2O_3 waveguides at different wavelengths and different input powers. (Insert: theoretical TPA coefficients) (c) Calculated sidewall scattering loss for β-Ga_2O_3 waveguides. (d) Calculated top surface scattering loss for β-Ga_2O_3 waveguides.